Contents lists available at ScienceDirect

Arabian Journal of Chemistry

journal homepage: www.ksu.edu.sa

Deciphering the potential therapeutic targets and mechanisms of jaranol for the treatment of COVID-19 and lung adenocarcinoma

Zhongcui Kang, Qian Wu, Qihang Peng, Yiting Deng, Hongxia Xu, Yu Xiao, Jingda Li, Shaobin Li, Jin Li *, Ying Chen *

College of Life Science, Yangtze University, Jingzhou 434025, China

ARTICLE INFO

Keywords:
Jaranol
COVID-19
Lung adenocarcinoma
Network pharmacology

ABSTRACT

Patients with lung adenocarcinoma (LUAD) are vulnerable to COVID-19. However, there is currently a lack of available treatments for LUAD patients infected with COVID-19. Jaranol is a naturally derived flavonoid that exhibits promising properties as an antiviral and antitumor agent. Therefore, this research intends to investigate the molecular targets and underlying mechanisms of jaranol for the treatment of COVID-19/LUAD. Through network pharmacology, 47 intersection target genes were identified for jaranol against COVID-19/LUAD, and an eight-gene risk score model with strong predictive accuracy for LUAD patients was constructed. Functional enrichment analysis demonstrated that the main mechanism of jaranol in combating COVID-19/LUAD involved the regulation of response to hormone, positive regulation of phosphorylation, and PI3K-Akt signaling pathway. Furthermore, the results of molecular docking analysis indicated that jaranol exhibited a significant affinity with eight hub targets (AKT1, SRC, EGFR, HSP90AA1, ESR1, PTGS2, PPARG, and MMP9) as well as three core COVID-19-related targets (ACE2, 3CLpro, and PLpro). The direct binding between jaranol and MMP9 was then validated in A549 lung cancer cells using cellular thermal shift assay (CETSA). These findings suggest that jaranol has a promising therapeutic effect against COVID-19/LUAD, providing a theoretical foundation and novel perspectives for future development as a potential pharmaceutical candidate.

1. Introduction

The global spread of the coronavirus disease 2019 (COVID-19), caused by the severe acute respiratory syndrome coronavirus 2 (SARS-CoV-2), has been swift and extensive since its occurrence in 2019, leading to significant rates of illness and death and becoming a critical global public health emergency. As of October 4, 2023, the World Health Organization (WHO) has received reports of over 770 million confirmed cases of COVID-19, with a staggering death toll exceeding 6.9 million (World Health Organization, 2023). Available data confirmed that patients with cancer, especially lung cancer (Luo et al., 2020), may be more susceptible to SARS-CoV-2 infection and that COVID-19 patients with underlying malignancies had a greater fatality rate than those without cancer (Lee et al., 2020). Lung cancer is the primary cause of cancer mortality, accounting for approximately 2.2 million newly diagnosed cases and 1.8 million fatalities in 2020 (Sung et al., 2021). Among the various subtypes of lung cancer, lung adenocarcinoma (LUAD) is the prevailing form. The current treatment for COVID-19 primarily consists of antiviral drugs, immunomodulator agents, neutralizing antibodies and convalescent plasma, and antithrombotic therapy (Andrews et al., 2024). These therapies have halted the progression of the disease and reduced the severity of symptoms and side effects; however, they have not yet achieved a complete cure. Several research studies have investigated the potential therapeutic benefits of natural compounds in the treatment of COVID-19 or lung cancer (Khan and Lee, 2023; Elkhalifa et al., 2023), but it is critical to recognize that there are currently no effective pharmaceutical interventions that simultaneously target both COVID-19 and LUAD.

Jaranol, also referred to as kumatakenin, is a naturally occurring flavonoid found in various herbs such as cloves, licorice (*Glycyrrhiza spp.*), and *Astragalus membranaceus* (Woo et al., 2017; Chen et al., 2021; Zhang and Huang, 2021). Previous studies have indicated that jaranol exhibits potential inhibitory activity against liver cancer, endometrial cancer, and ovarian cancer (Mo et al., 2023; Zhang and Huang, 2021; Woo et al., 2017). Additionally, jaranol has been found to effectively inhibit the release and transmission of the influenza virus by targeting

* Corresponding authors at: College of Life Science, Yangtze University, No. 266 Jingmi Road, Jingzhou, Hubei Province 434025, China.
E-mail addresses: lijin28@yangtzeu.edu.cn (J. Li), chenyingcy@yangtzeu.edu.cn (Y. Chen).

https://doi.org/10.1016/j.arabjc.2024.105648
Received 11 October 2023; Accepted 22 January 2024
Available online 24 January 2024

neuraminidase (Ling et al., 2023). Furthermore, jaranol has demonstrated anti-SARS-CoV-2 effects in human lung adenocarcinoma cells (Leal et al., 2021). Nevertheless, there is still a deficiency of studies examining the underlying mechanism of jaranol in treating COVID-19 patients with lung cancer. Therefore, the present study aims to utilize network pharmacology and various computational biological approaches to conduct a comprehensive analysis of the potential targets and mechanisms of jaranol against COVID-19/LUAD. These findings will be further validated through molecular docking and CESTA experiments. The detailed strategy is illustrated in Fig. 1.

2. Materials and methods

2.1. Identification of jaranol-related genes

We used the TCMSP database (https://old.tcmsp-e.com/tcmsp.php) (Ru et al., 2014), HERB database (https://herb.ac.cn/) (Fang et al., 2021), SwissTargetPrediction database (www.swisstarget prediction.ch/) (Daina et al., 2019), Similarity ensemble approach (SEA, https://sea.bkslab.org/) (Keiser et al., 2007), ETCM database (https://www.tcmip.cn/ETCM/index.php/Home/) (Xu et al., 2019), PharmMapper database (https://www.lilab-ecust.cn/pharmmapper/) (Wang et al., 2017), and SymMap database (https://www.symmap.org/) (Wu et al., 2019) to identify potential therapeutic targets of jaranol, and to ensure the precision of following analysis, genes appearing at least twice in seven databases were considered to be jaranol-related targets. The jaranol targets were displayed using the Evenn website at https://www.ehbio.com/test/venn/.

2.2. Identification of COVID-19/LUAD-related genes

We used the R software 'DESeq2' package to evaluate the differentially expressed genes (DEGs) from the transcriptome sequencing data of TCGA-LUAD (https://portal.gdc.cancer.gov/) and GEO136043 dataset (https://www.ncbi.nlm.nih.gov/geo/). The screening parameters were $P < 0.01$ and $|\log2(\text{fold change})| \geq 2$. Furthermore, we also conducted a search in various databases including Comparative Toxicogenomics Database (CTD, https://ctdbase.org/), DisGeNET (https://www.disgenet.org/), GeneCards (https://www.genecards.org), Malacards (https://www.malacards.org/), PubChem (https://pubchem.ncbi.nlm.nih.gov/), and OMIM (https://omim.org/), using the keyword "lung adenocarcinoma" to identify potential target genes. COVID-19-related genes were obtained from seven databases, namely CTD, DisGeNET, GeneCards, Malacards, PubChem, OMIM, and KEGG (https://www.kegg.jp/kegg/disease/). In all databases, genes that appeared at least twice were deemed to be associated with LUAD or COVID-19.

2.3. Acquisition and clinical prognostic analysis of intersection genes for jaranol and COVID-19/LUAD

We utilized the Evenn website to determine the intersection genes that are associated with jaranol, and COVID-19/LUAD. Using the "glmnet" package, we performed multivariate Lasso Cox regression on intersecting genes based on ten-fold cross-validation to obtain regression-significant genes. A risk score model was constructed, and patients were classified into high- and low-risk subgroups according to the median risk score to determine the prognosis of the signature. Then the overall survival (OS) time was compared between two subgroups with the use of the R package "survival", and the risk score curve was visualized with the "ggplot2" package. To assess predictive value, receiver operating characteristic (ROC) curves (containing 1-year, 3-year, and 5-year survival) were created using the "timeROC" package.

2.4. Functional enrichment analysis of common target genes

We used the Metascape database (https://metascape.org/) (Zhou et al., 2019) to perform Gene Ontology (GO) and Kyoto Encyclopedia of Genes and Genomes (KEGG) pathway enrichment analysis (Kanehisa

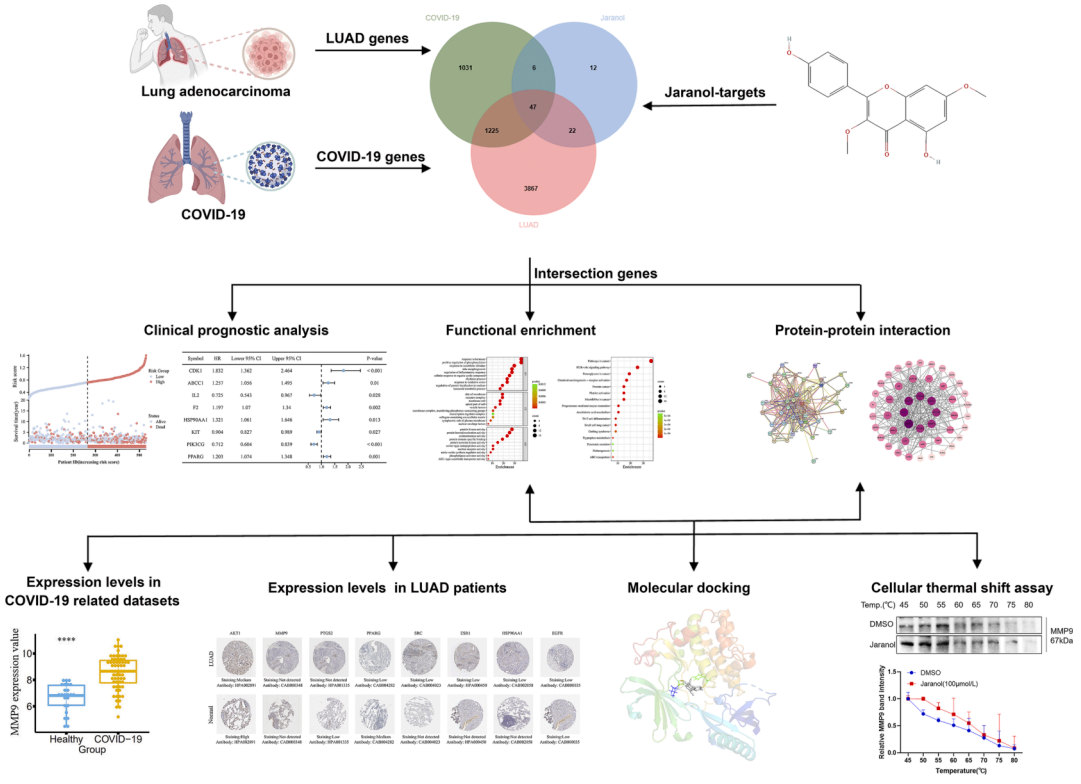

Fig. 1. The graphical abstract of this study. The figure shows the process of deciphering the molecular mechanism of jaranol against COVID-19/LUAD using network pharmacology, bioinformatics analysis, and CETSA.

et al., 2017), with the *P* value set to 0.01. The GO enrichment analysis includes cellular composition (CC), molecular function (MF), and biological processes (BP). The results were visualized on an online platform (https://www.bioinformatics.com.cn).

2.5. Protein-protein interaction (PPI) network construction and analysis

For generating the PPI network, the intersection targets were imported into the STRING database (https://string-db.org) with a minimal interaction threshold (medium confidence) set at 0.4000, and the species was defined as "*Homo sapiens*" (Szklarczyk et al., 2021). Cytoscape 3.9.1 software (https://cytoscape.org/) was applied to illustrate the PPI network.

2.6. Expression levels of hub genes in COVID-19 or LUAD patients

The COVID-19db (https://hpcc.siat.ac.cn/covid19db/home) database was used to examine the expression differences of hub genes in COVID-19 patients. The GSE152641 and GSE171110 datasets included RNA-seq data from 62 COVID-19 patients and 24 healthy controls, and 44 COVID-19 patients and 10 healthy controls, respectively. To validate the mRNA expression of hub genes in LUAD patients, we employed data from TCGA-LUAD through the R software package "ggplot2". Additionally, the immunohistochemistry images of hub proteins were sourced from the Human Protein Atlas (HPA) (Uhlen et al., 2017).

2.7. Molecular docking analysis

The molecular structures of jaranol, baritinib, and remdesivir (Supplementary Fig. S1) were retrieved from the TCMSP database and saved in mol2 format. The 3D structures of target proteins were downloaded from the RCSB PDB Protein structure database (https://www.rcsb.org/). To prepare the structures for docking, all water molecules and original ligands were eliminated using PyMOL 2.4.0 software (https://pymol.org/2/). AutoDockTools 1.5.7 (https://autodock.scripps.edu/) was employed for hydrogenation and conversion of the structures to PDBQT format. Docking simulations were performed using the AutoDock Vina program. Subsequently, the model with the lowest binding energy was selected for visual analysis by by PyMOL 2.4.0 software (https://pymol.org/2/).

2.8. Cellular thermal shift assay (CETSA)

Human non-small cell lung cancer A549 cells were obtained from Beijing Institute of Basic Medical Sciences, and maintained in DMEM medium containing 10 % fetal bovine serum (FBS) (Gibco, Carlsbad, USA), at 37 ℃, 5 % CO_2 incubator. A549 cells were seeded into a six-well plate at a density of 1×10^6 cells// well. After 24 h, the cells were washed twice with PBS and lysed with RIPA buffer containing a complete protease inhibitor mixture (Beyotime, Shanghai, China) for 20 min. Subsequently, the cell lysate was centrifuged at 12,000 g for 15 min at 4 ℃, the supernatants were collected and divided into two equal parts, and incubated with 100 μM jaranol (Chemfaces, Wuhan, China) or DMSO control for 1 h, respectively. Each lysate was further divided into eight equal parts (100 μL) and heated at different temperatures (45, 50, 55, 60, 65, 70, 75, and 80 °C) for 5 min, followed by cooling at room temperature for 5 min. After centrifugation, the supernatant was collected for the analysis of MMP9 levels using Western blot. Primary antibodies against MMP9 (1:1000 dilution) and secondary antibodies (1:2000 dilution) were obtained from Proteintech (Wuhan, China).

2.9. Statistical analysis

The data were presented as the mean ± standard deviation (SD). A Student's *t*-test was performed to assess the differences between the two groups using GraphPad Prism 9.0 software. The value of $P < 0.05$ was considered statistically significant.

3. Results

3.1. Determination of common targets for jaranol, COVID-19, and LUAD

By searching multiple databases and using occurrences in at least two databases as screening criteria, we identified therapeutic genes associated with jaranol, COVID-19, and LUAD. Our search yielded a total of 19, 77, 13, 100, 51, 23, and 284 jaranol-associated target genes from the HERB, TAE, TCMSP, SwissTargetPrediction, ECTM, SymMap, and PharmMapper databases, respectively (Fig. 2A). After applying our screening criteria, we identified a total of 87 therapeutic target genes for jaranol (Fig. 2A). Furthermore, we performed differential gene expression analysis on the TCGA-LUAD and GSE136043 datasets. In the GSE136043 dataset, 1328 up-regulated and 1185 down-regulated genes were identified (Fig. 2B), whereas 3128 up-regulated genes and 748 down-regulated genes in the TCGA-LUAD database (Fig. 2C), resulting in the identification of 2513 and 3876 LUAD-associated genes, respectively. Additionally, we retrieved 8750, 2438, 5627, 116, 7, and 200 genes related to LUAD from the CTD, DisGeNET, GeneCards, Malacards, PubChem, and OMIM databases, respectively. Through this process, we screened out a total of 5161 therapeutic target genes for LUAD (Fig. 2D). Moreover, we retrieved 2309 COVID-19-related genes from the CTD, DisGeNET, GeneCards, KEGG, Malacards, OMIM, and PubChem databases (Fig. 2E). Ultimately, we utilized the Evenn website to determine 47 intersection genes that are associated with jaranol, COVID-19, and LUAD (Fig. 2F, Supplementary Table S1).

3.2. Clinical prognostic analysis of COVID-19/LUAD-related genes

We investigated the relationship between the 47 intersection genes mentioned above and the prognosis of COVID-19/LUAD patients. Through Lasso-Cox regression analysis, we identified 10 significant genes (Fig. 3A, B). Subsequently, a risk score model consisting of eight genes was established using multivariate Cox regression analysis, including *CDK1*, *ABCC1*, *IL2*, *F2*, *HSP90AA1*, *KIT*, *PIK3CG*, and *PPARG* (Fig. 3C). Based on their risk scores, patients were separated into high- and low-risk groups. The risk curve and Kaplan-Meier survival analysis demonstrated that high-risk patients had a significantly higher mortality rate and shorter overall survival (OS) compared to low-risk individuals (Fig. 3D, E). Additionally, we evaluated the accuracy and reliability of the risk score using ROC curve analysis, which determined that the AUCs for 1-, 3-, and 5-year OS were 0.697, 0.654, and 0.686, respectively (Fig. 3F), indicating the reliable diagnostic applicability of this gene signature.

3.3. Functional enrichment analysis of common target genes

Subsequently, we analyzed the functional enrichment of the common target genes using the Metascape database. The results obtained from the Gene Ontology (GO) analysis revealed several significant biological process (BP) terms, including response to hormone, positive regulation of phosphorylation, response to xenobiotic stimulus, tube morphogenesis, and regulation of inflammatory response (Fig. 4A). Additionally, the top cellular component (CC) terms identified were side of the membrane, receptor complex, membrane raft, apical part of cell, and vesicle lumen (Fig. 4A). Furthermore, the top molecular function (MF) terms were found to be protein kinase activity, protein homodimerization activity, oxidoreductase activity, protein domain specific binding, and protein tyrosine kinase activity (Fig. 4A). Moreover, the KEGG enrichment analysis indicated that most genes were involved in essential biological pathways such as pathway in cancer, PI3K-Akt signaling pathway, proteoglycans in cancer, chemical carcinogenesis-receptor activation, prostate cancer, platelet activation, microRNAs in cancer, progesterone-mediated oocyte maturation, arachidonic acid

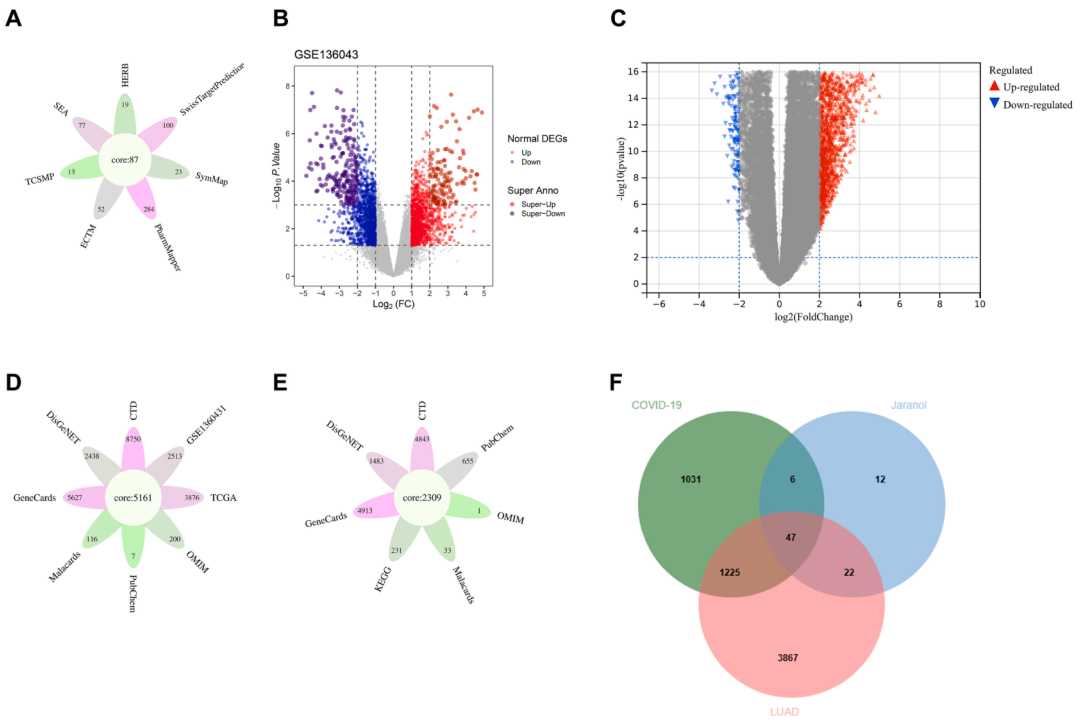

Fig. 2. Potential target genes of jaranol for the therapy of COVID-19/LUAD complication. (A) Target genes correlated with jaranol in seven different databases. (B) Volcano plot of DEGs in LUAD from the GSE136043 dataset. (C) Volcano plot of DEGs in LUAD from the TCGA dataset. (D) LUAD-related genes. (E) COVID-19-related genes in seven databases. (F) Venn diagram of therapeutic target genes of jaranol, COVID-19/LUAD.

metabolism, Th17 cell differentiation, and small cell lung cancer (Fig. 4B).

3.4. PPI network construction and analysis

We generated a protein–protein interaction (PPI) network on the basis of the STRING database using 47 jaranol common target genes against COVID-19/LUAD (Fig. 5A) and then imported the network into Cytoscape for further analysis. Therefore, a PPI network was created with 47 nodes, 277 edges, and an average degree value of 11.8 for each protein (Fig. 5B). Finally, eight hub genes were identified according to topological parameters and degree value, namely *AKT1*, *SRC*, *EGFR*, *HSP90AA1*, *ESR1*, *PTGS2*, *PPARG* and *MMP9* (Fig. 5C).

3.5. Expression levels of hub genes in COVID-19-related datasets

In order to investigate the mRNA expression differences of eight hub genes between individuals with COVID-19 and healthy control groups, we analyzed the GSE152641 and GSE171110 datasets. As presented in Figs. 6 and 7, in both datasets, the expression level of *AKT1* was significantly higher in the healthy control group compared to the COVID-19 group. Conversely, *MMP9* and *PPARG* exhibited significantly lower expression levels in the healthy control group, while no significant difference was observed in the expression of *ESR1*. In the GSE171110 dataset, no significant difference in the expression of *PTGS2* was observed, whereas in the GSE152641 dataset, a noticeable down-regulation was found in the healthy control group. Additionally, in the GSE171110 dataset, the expression levels of *SRC*, *HSP90AA1*, and *EGFR* were markedly elevated in the healthy control group, while no significant variation was observed in the GSE152641 dataset.

3.6. The expression levels of hub genes in LUAD patients

We utilized the TCGA database to examine the expression levels of eight hub genes in LUAD patients. The findings revealed that, in comparison to normal tissues, the mRNA expression levels of *MMP9*, *SRC*, and *HSP90AA1* were markedly increased in LUAD, whereas *AKT1*, *PTGS2*, and *PPARG* were significantly reduced. No significant alterations were observed for *ESR1* and *EGFR* (Fig. 8A). The protein expression levels of AKT1, PPARG, and EGFR in the HPA database were consistent with the aforementioned mRNA expression levels (Fig. 8B). However, the protein levels of MMP9 were not detected in both LUAD and normal lung tissues. Similarly, the protein level of PTGS2 was not observed in LUAD tissues but at a low level in normal lung tissues. Conversely, the low protein levels of SRC, ESR1, and HSP90AA1 were observed in LUAD tissues, but with not detected in normal lung tissues (Fig. 8B).

3.7. Molecular docking analysis

Molecular docking was conducted using AutoDock Vina software to assess the binding affinity of jaranol with eight hub targets. The obtained results are presented in Table 1 and Fig. 9. The calculated binding energies between jaranol and the eight hub proteins were all not more than −7.5 kcal/mol, indicating a strong binding capacity of jaranol. Notably, the molecular docking analysis revealed that the interaction between jaranol and AKT1 exhibited the lowest binding energy (−9.5 kcal/mol), followed by MMP9 (−9.3 kcal/mol), PTGS2 (−8.4 kcal/mol), PPARG (−8.2 kcal/mol), and SRC (−8.2 kcal/mol). To further evaluate the potential mechanism of action of jaranol in the treatment of COVID-19, additional molecular docking experiments were performed. In this analysis, jaranol was subjected to dock with three COVID-19-related targets, namely ACE2, 3CLpro, and PLpro, while two FDA-approved medicines, baritinib, and remdesivir served as positive controls. The results, presented in Table S2 and Fig. S2, demonstrated that jaranol exhibited the lowest binding energy with PLpro (−7.6 kcal/mol), followed by ACE2 (−7.5 kcal/mol), and 3CLpro (−7 kcal/mol). Importantly, the binding energies of jaranol with PLpro and 3CLpro were lower than those of the control drugs baritinib and remdesivir. These findings implied that jaranol deserved further investigation as a

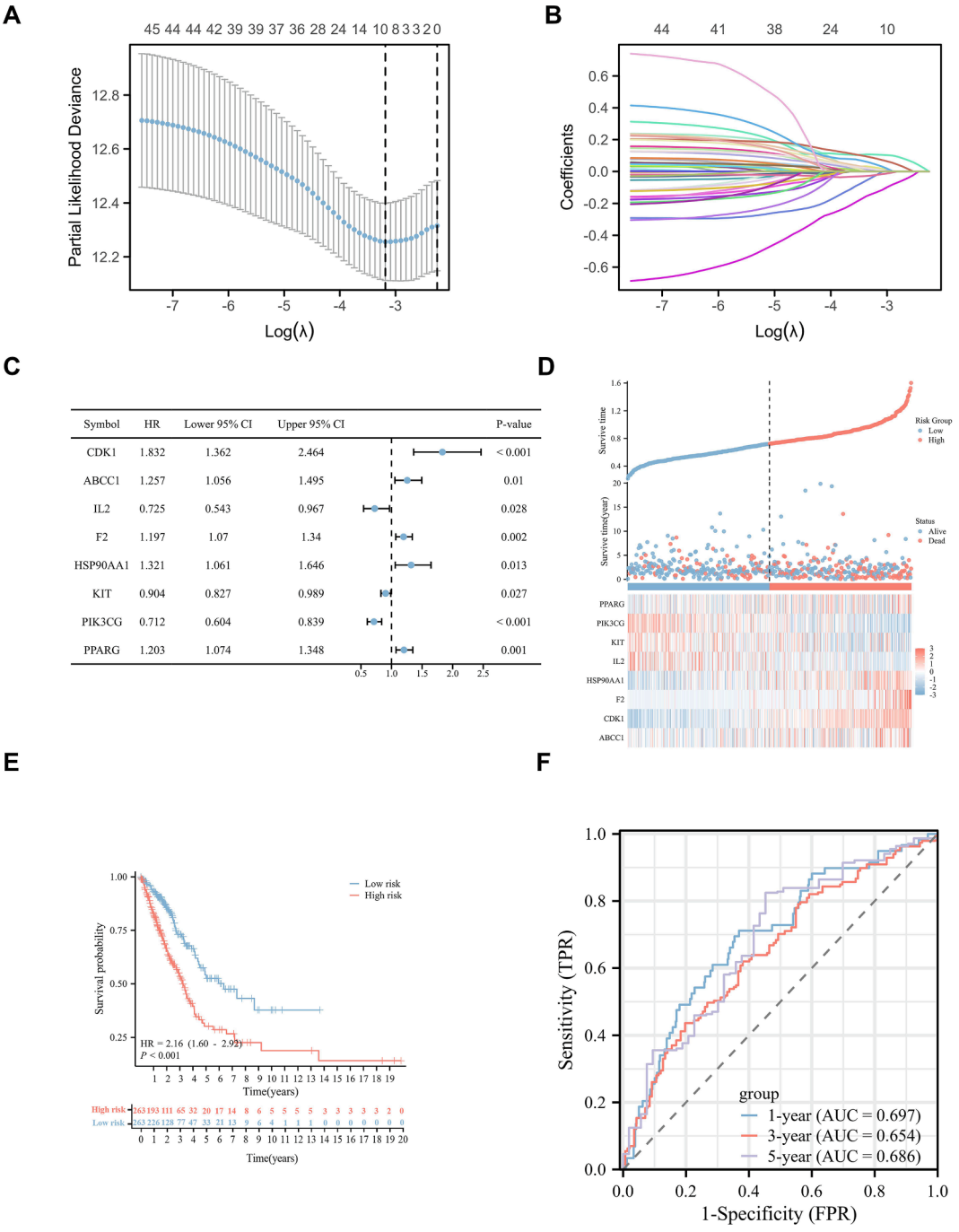

Fig. 3. Prognostic model and survival analysis of patients with LUAD. (A) Coefficient curve determined by LASSO regression analysis for LUAD. (B) Plot of cross-validation error rate for LASSO regression analysis of LUAD. (C) Multivariate Cox analysis presented in a forest plot. (D) The median risk scores and survival status distributions. (E) Kaplan-Meier analysis for high- and low-risk groups. (F) ROC curves of the risk score.

potential treatment for COVID-19.

3.8. Jaranol directly binds to MMP9 in A549 cells

Given the significant upregulation of MMP9 in patients with COVID-19 or LUAD, as well as its strong affinity for jaranol (with a binding energy of −9.3 kcal/mol), we employed the cellular thermal shift assay (CETSA) to investigate the direct binding between jaranol and MMP9 in A549 cells. The results, depicted in Fig. 10, demonstrated a gradual reduction in the expression of MMP9 protein as the temperature increased from 45 to 80 °C. Notably, following incubation with 100 μM jaranol, the thermal stability of MMP9 protein in A549 cells was considerably higher than that of the control group treated with DMSO alone. These findings suggested that jaranol was capable of directly binding to MMP9.

4. Discussion

In this study, we investigated the possible molecular mechanism of jaranol in the treatment of COVID-19 and LUAD comorbidity. 47 common jaranol target genes were identified in the therapeutic approach for COVID-19/LUAD through network pharmacology, and a risk score model with good predictive performance was established. Functional enrichment analysis revealed that jaranol primarily exerted its effects

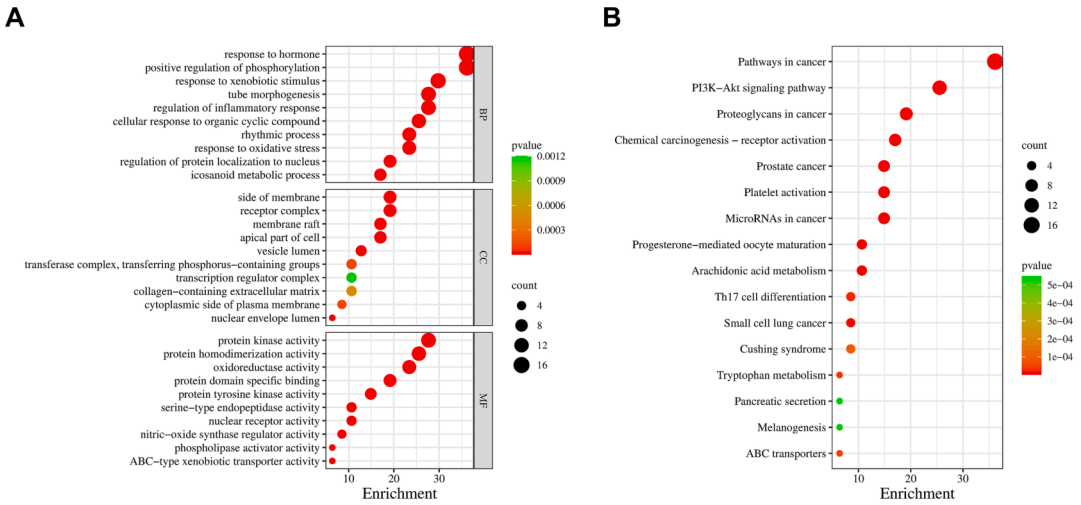

Fig. 4. GO and KEGG enrichment analysis of potential therapeutic target genes of jaranol against COVID-19/LUAD. (A) GO enrichment analysis. (B) KEGG pathway enrichment analysis.

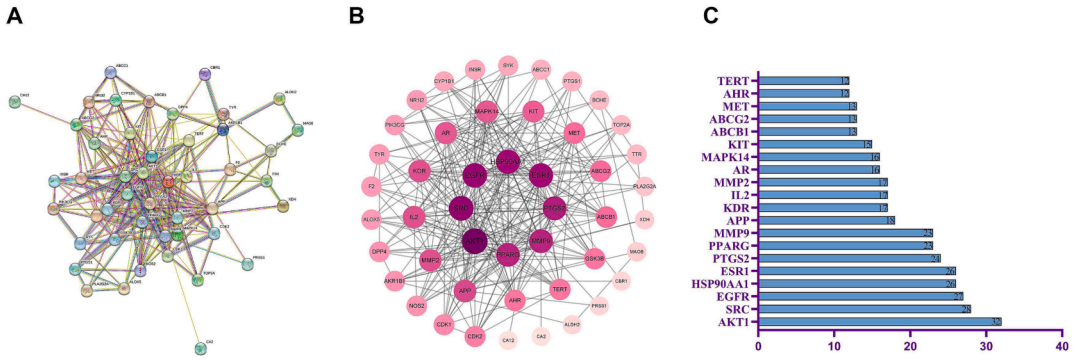

Fig. 5. PPI network of hub target genes for jaranol against COVID-19/LUAD. (A) PPI networks from the STRING database. (B) PPI networks were constructed using the node degree values. The degree of the node is proportional to the depth of the node color. (C) The top 20 core proteins were plotted according to the size of the node.

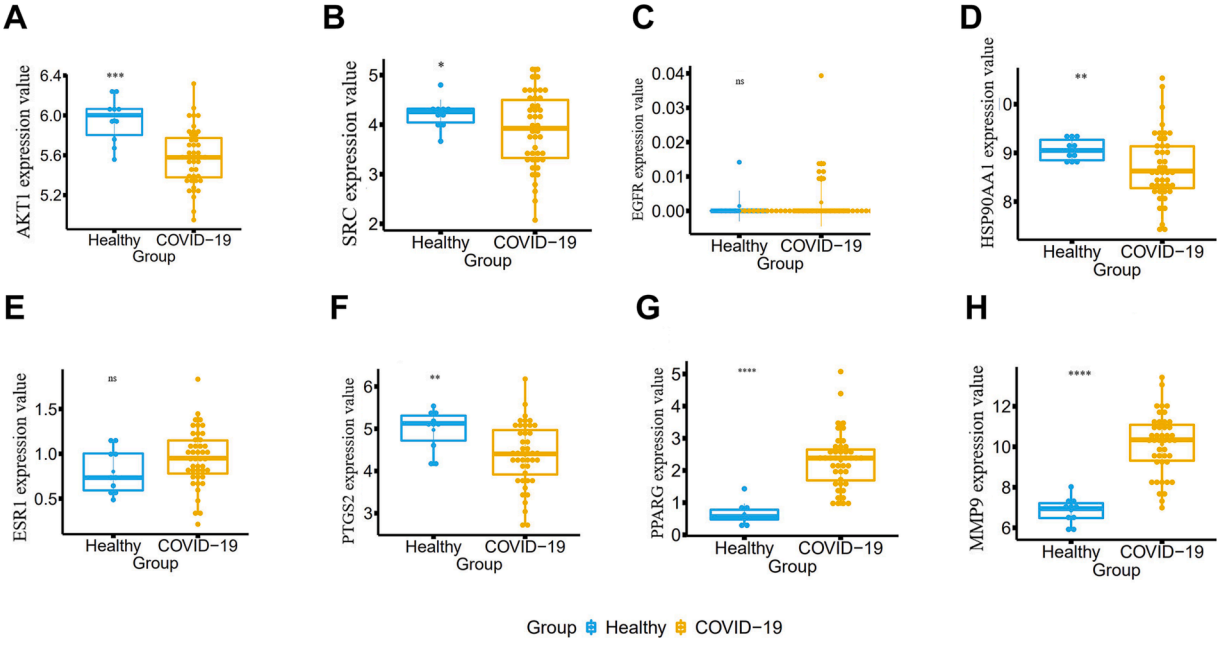

Fig. 6. Expression levels of the hub genes in the GSE152641 dataset. (A) *AKT1*. (B) *SRC*. (C) *EGFR*. (D) *HSP90AA1*. (E) *ESR1*. (F) *PTGS2*. (G) *PPARG*. (H) *MMP9*. The expression value was presented as the mean ± standard deviation (SD). * $P < 0.05$, ** $P < 0.01$, *** $P < 0.001$. ns, no significance.

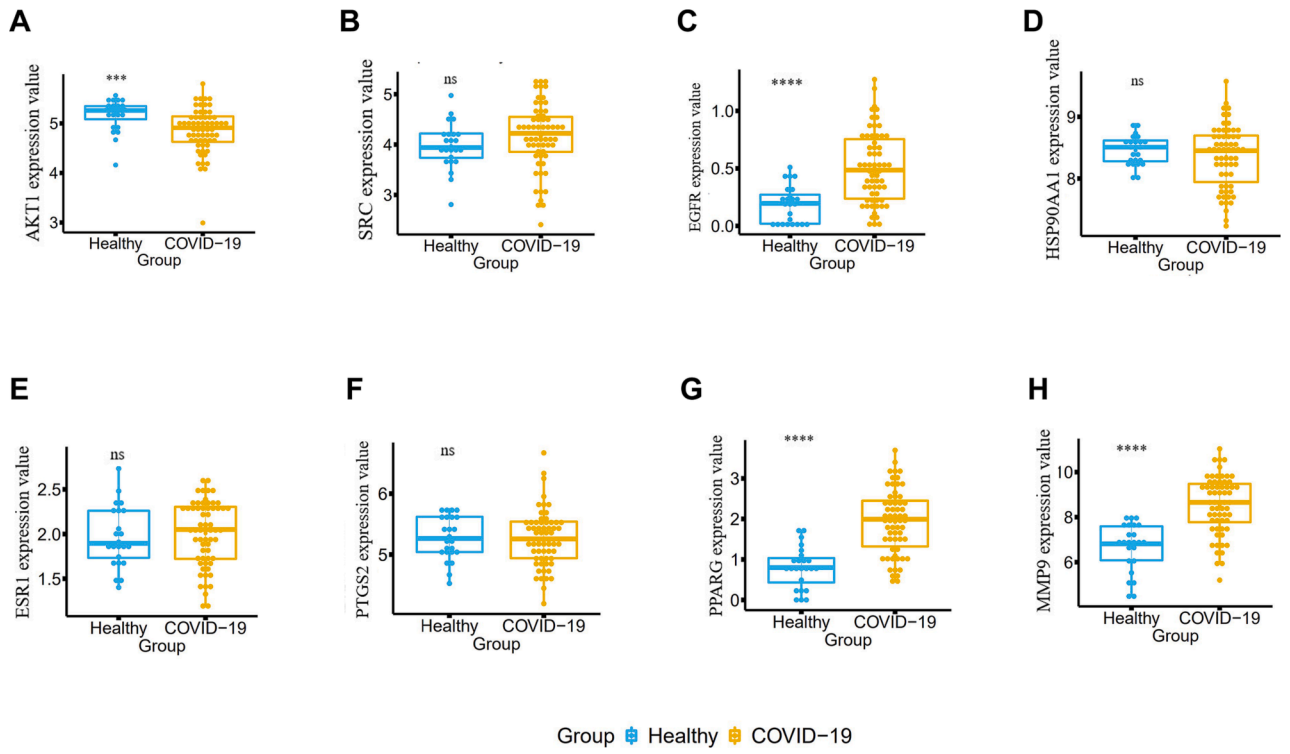

Fig. 7. Expression levels of the hub genes in the GSE171110 dataset. (A) *AKT1*. (B) *SRC*. (C) *EGFR*. (D) *HSP90AA1*. (E) *ESR1*. (F) *PTGS2*. (G) *PPARG*. (H) *MMP9*. The expression value was presented as the mean ± standard deviation (SD). *** $P < 0.001$, **** $P < 0.0001$. ns, no significance.

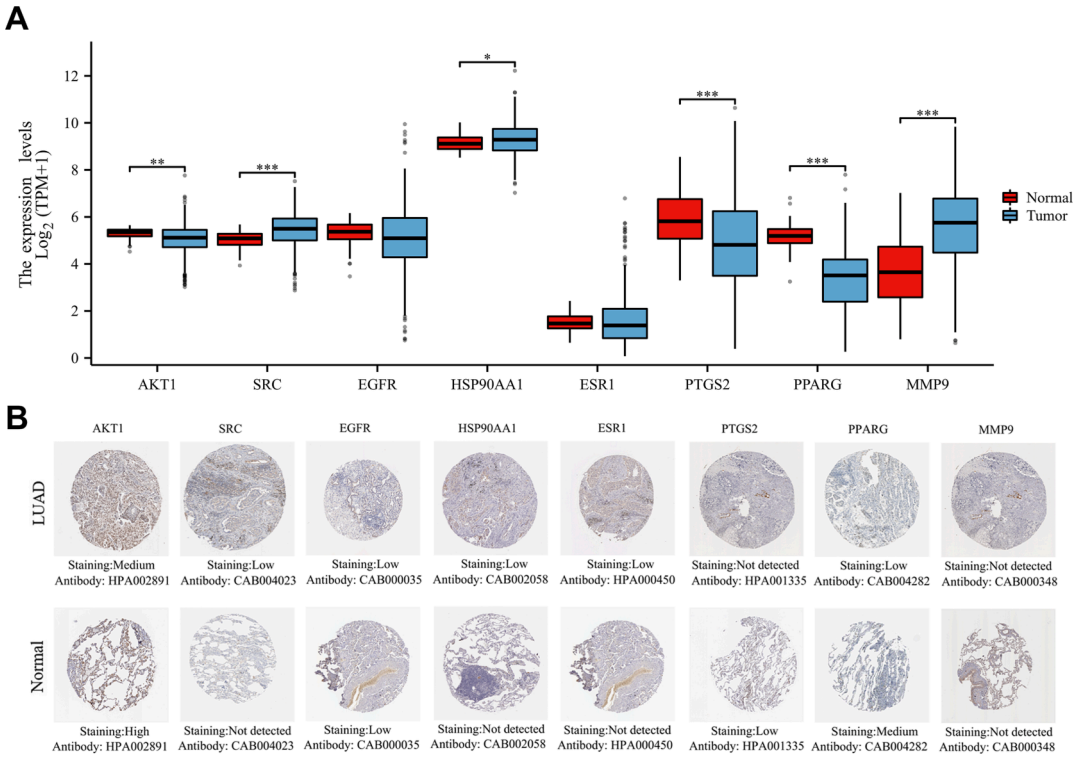

Fig. 8. Expression levels of hub genes in LUAD patients. (A) Differential mRNA expression of hub genes between LUAD tissues and adjacent non-tumor tissues based on TCGA dataset. (B) The protein expression of hub genes in LUAD tissues and normal lung tissues according to the HPA database. The expression levels were presented as the mean ± standard deviation (SD). * $P < 0.05$, ** $P < 0.01$, *** $P < 0.001$.

through the modulation of response to hormone, positive regulation of phosphorylation, and PI3K-Akt signaling pathway against COVID-19/LUAD. Moreover, eight hub target genes were obtained according to PPI network analysis, including *AKT1*, *SRC*, *EGFR*, *HSP90AA1*, *ESR1*, *PTGS2*, *PPARG*, and *MMP9*.

KEGG enrichment analysis showed that the 47 intersection genes

Table 1
Docking analysis of eight hub proteins of COVID-19/LUAD with jaranol.

Protein target	Uniprot ID	PDB ID	Affinity (kcal/mol)	Interacting residues
AKT1	P31749	7NH5	−9.5	TYR-272, SER-205, ASN-204
MMP9	P14780	4HMA	−9.3	ARG-249, GLU-241, HIS-257
PTGS2	P35354	5IKT	−8.4	TYR-130
PPARG	P37231	6MS7	−8.2	GLU-295
SRC	P12931	7NG7	−8.2	LYS-298, THR-341
ESR1	P03372	1XPC	−7.5	VAL-534, ASN-532, TYR-526, LEU-536,
HSP90AA1	P07900	5XRD	−7.5	LEU-107, ASN-51
EGFR	P00533	5UG9	−7.5	MET-793

were mainly concentrated in the PI3K-Akt signaling pathway. It has been demonstrated that the PI3K-Akt signaling pathway regulates a clathrin-mediated mechanism that facilitates the endocytosis of SARS-CoV-2 (Basile et al., 2022). Conversely, the SARS-CoV-2 S protein was found to inhibit inflammatory reactions in alveolar epithelial type II cells during the initial phases of infection by activating the PI3K-Akt pathway (Al-Qahtani et al., 2022). In non-small cell lung cancer (NSCLC), the PI3K/Akt/mTOR pathway has been strongly associated with both tumorigenesis and the development of disease, being essential for controlling several cellular functions such as angiogenesis, metastasis, proliferation, and migration (Sanaei et al., 2022). In fact, inhibitors targeting the PI3K-Akt pathway have demonstrated potential anti-SARS-CoV-2 effects. For instance, the PI3K inhibitor VPS34-IN1 and its bioavailable analogue VVPS34-IN1 have exhibited strong inhibitory effects on SARS-CoV-2 infection in human lung tissue cultures (Yuen et al., 2021). Furthermore, a number of specific inhibitors targeting PI3K and Akt are presently undergoing development and evaluation in preclinical studies and early-stage clinical trials for NSCLC (Tan, 2020). Consequently, it is postulated that jaranol may potentially play a role in the treatment of COVID-19 and LUAD by modulating the PI3K-Akt pathway. AKT1, also known as protein kinase B, is a serine/threonine protein kinase that needs to be activated by the PI3K pathway (Franke et al., 1995). A recent study indicated a remarkable reduction in viral production when treating SARS-CoV-2-infected Huh7 cells with Akt inhibitors (Appelberg et al., 2020). Furthermore, Akt inhibition may boost regulatory T cells (Tregs) in the lungs of COVID-19 patients, thereby decreasing inflammation and facilitating damage resolution (Appelberg et al., 2020). In lung cancer, AKT contributes a crucial function in malignant development and metastasis. Both AKT and the activated form of Akt (phosphorylated Akt, p-Akt) were found to be overexpressed in NSCLC tumor tissues, which correlated with a poor prognosis (Tang et al., 2006; Yuan et al., 2015). The tyrosine-protein kinase SRC was determined to be associated with several COVID-19-related pathophysiological pathways (Tomazou et al., 2021), and a recent study demonstrated that Bafetinib (an SRC inhibitor) decreased SARS-CoV-2 titers in a dose-dependent way (Meyer et al., 2021). Abnormal expression and activity of SRC were reported in more than 50 % of NSLC patients (Mazurenko et al., 1992). SRC can affect several downstream carcinogenic growth factor receptors, and inhibition of SRC

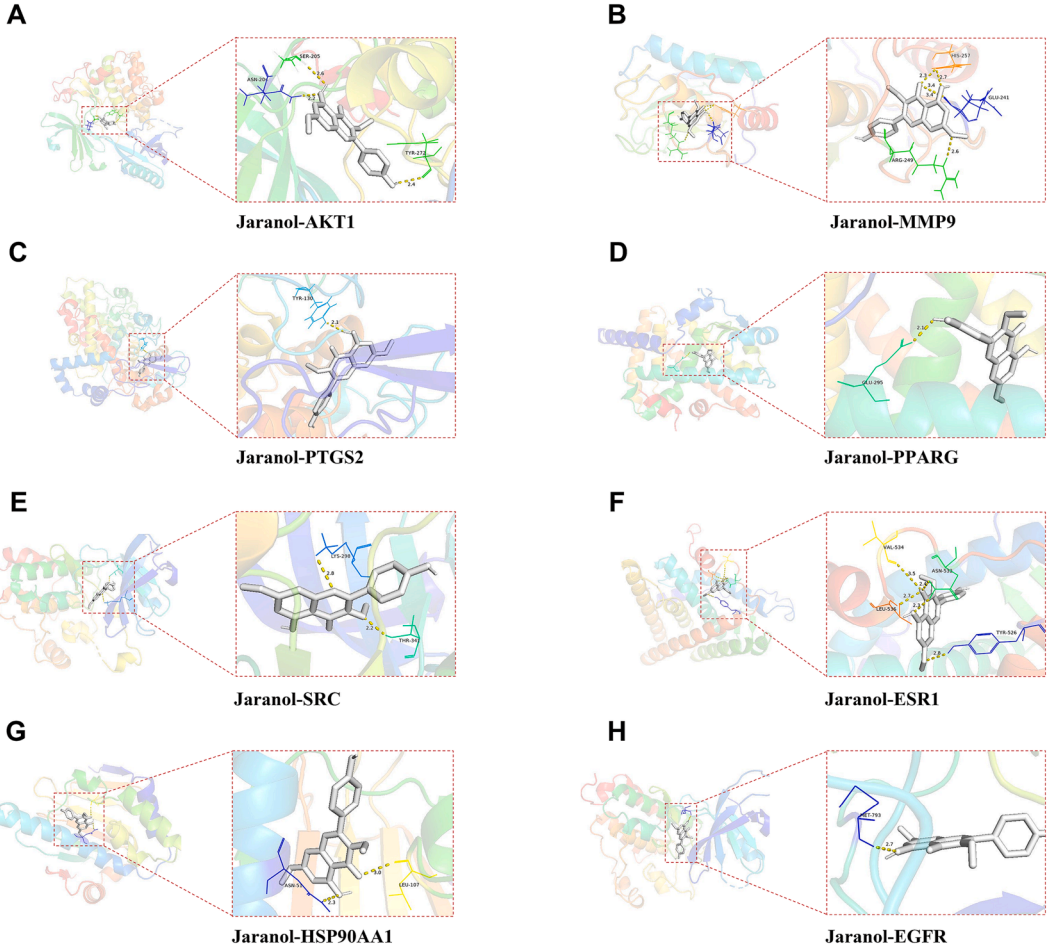

Fig. 9. Molecular docking diagram of jaranol against the hub targets of COVID-19/LUAD. (A) AKT1. (B) MMP9. (C) PTGS2. (D) PPARG. (E) SRC. (F) ESR1. (G) HSP90AA1. (H) EGFR. The colors represent the amino acid residues of proteins that are bound to small molecule ligands, while white and gray indicate the small molecule ligands. In addition, yellow dashed lines denote the presence of hydrogen bonds.

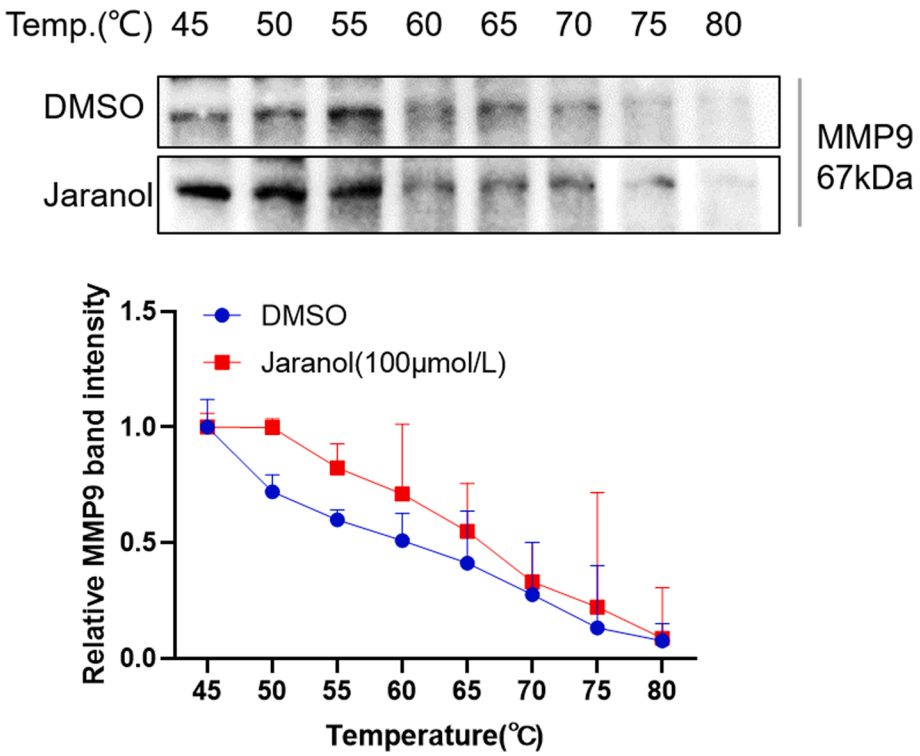

Fig. 10. CETSA analysis of the binding interaction between jaranol and MMP9. A549 cells were treated with jaranol at a concentration of 100 μM, while DMSO was used as a control. The effect of Jaranol on the stability of MMP9 protein was assessed through Western blotting.

is a viable treatment for advanced NSCLC (Giaccone and Zucali, 2008). EGFR, the tyrosine kinase receptor required for inflammatory cell activation and proliferation, would be elevated in the SARS-CoV-2-infected lung after acute lung damage (Matsuyama et al., 2020). In the development of NSCLC, EGFR, recognized as a cancer driver gene, exhibits various carcinogenic effects such as cell cycle, cell proliferation, cell metastasis, and invasion (Liu et al., 2017). The blockade of EGFR could be recommended as an appealing and potential target for both NSCLC and COVID-19 patients (Londres et al., 2022, Herrera-Juárez et al., 2023). A recent study has shown that inhibition of HSP90AA1 activity directly suppressed virus production and attenuated inflammatory damage by preventing SARS-CoV-2-induced pyroptosis (Zhao et al., 2023). The AKT1/ERK pathway was similarly suppressed by HSP90AA1 knockdown, which reduced lung cancer cell growth and triggered apoptosis in mouse and human lung cancer cell lines (Niu et al., 2021). ESR1 is an important sex factor that protects COVID-19 patients by decreasing the immunological and inflammatory responses caused by SARS-CoV-2 infection (Li et al., 2022). The expression of ESR1 in lung cancer was linked to the decrease of epithelial-mesenchymal transition (EMT) markers, and also an independent prognostic factor for the prognosis of surgically resected patients with non-small cell lung cancer (Brueckl et al., 2013, Atmaca et al., 2015). PTGS2, also known as cyclooxygenase 2 (COX2), is an inducible proinflammatory molecule. Patients with the most severe types of COVID-19 exhibit extreme overexpression of COX2 as a result of SARS-CoV-2 infection (Perico et al., 2023). Additionally, an increased expression of COX2 could make COVID-19 patients more susceptible to morbidity and mortality (Passos et al., 2022). Recent studies have demonstrated COX-2 as an effective therapeutic target considering it is up-regulated and can contribute to the progression, angiogenesis, and metastasis of lung cancer. According to preclinical evidence, targeted COX-2 inhibition improves tumor response and survival, lowers cancer cell proliferation, and triggers cancer cell death. (Liu et al., 2015). PPARG, a ligand-activated transcription factor, has been proven to have promising anti-inflammatory effects by suppressing crucial inflammatory factors (particularly NF-B and AP-1), hence modulating inflammation in response to SARS-CoV-2 infection (Hasankhani et al., 2023). The activation of PPARG prevents primary tumor growth and metastases in lung cancer by altering cancer cell differentiation, proliferation, apoptosis, and motility, as well as making the tumor microenvironment less favorable to tumor growth and metastasis (Reddy et al., 2016, Shi et al., 2020). MMP9, a member of the matrix metalloproteinase (MMP) family, is intimately connected with angiogenesis, metastasis, and tumor growth for its ability to degrade extracellular matrix (ECM) proteins (Mondal et al., 2020). The presence of significantly higher MMP9 levels was found in the serum and lung tissue of severe COVID-19 patients (Hazra et al., 2020, Savic et al., 2022). MMP9 was also involved in inflammation, modulating the synthesis and release of cytokines and chemokines, implying a connection with COVID-19(Mondal et al., 2020). Moreover, MMP9 levels were dramatically increased and closely linked with metastasis in NSCLC patients, suggesting that it could be used as a possible biomarker for NSCLC to differentiate between normal and malignant conditions (Kowalczyk et al., 2023). These findings indicated that the therapeutic benefits of jaranol in treating COVID-19/LUAD may be attributed to its ability to hinder viral replication and infection, regulate inflammation and immune response, inhibit tumor progression, and modify the immune microenvironment of tumor cells by targeting these hub genes.

Furthermore, based on the molecular docking analysis, the binding energies between jaranol and the targets were all not more than −7.5 kcal/mol, indicating that jaranol exhibited high binding ability with eight hub targets. Meanwhile, we also observed that jaranol exerted good binding capacity with three COVID-19-related targets, namely ACE2, 3CLpro, and PLpro, and the binding energies were all not greater than −7.0 kcal/mol. ACE2 has been recognized as an entry receptor for SARS-CoV-2 (Wang et al., 2020). 3CLpro and PLpro, two viral proteases encoded by the SARS-CoV-2 genome, play a vital role in cleaving viral polyproteins and facilitating viral replication (Moustaqil et al., 2021). These proteases, along with ACE2, are widely acknowledged as crucial targets for COVID-19 therapy (Wu et al., 2020). Additionally, based on the upregulation of expression levels in both COVID-19 and LUAD, we

selected MMP9 to validate the binding capacity with jaranol by CETSA. As the temperature was elevated from 45 °C to 80 °C, the expression of MMP9 in the jaranol group exhibited a statistically significant increase when compared to that in the control group, suggesting that jaranol could bind directly to MMP9 (Fig. 10). MMP-9 has been identified as a potential early predictor of respiratory failure in COVID-19 patients (Ueland et al., 2020). In severe cases of COVID-19, the dysregulation of endocrine signaling pathways, including IGF1 and HGF, as well as aberrant activation of neutrophils, have been associated with the increased expression of MMP9. Furthermore, MMP9 has been implicated in the modulation of mitochondria-related processes and the advancement of COVID-19 disease (Wang et al., 2023). The significant upregulation of MMP9 also plays a crucial role in facilitating the migration and invasion of non-small cell lung cancer cells (Ge et al., 2023). Hence, the potential impact of jaranol in the binding and regulation of MMP9 could be highly significant in the therapeutic management of COVID-19 and LUAD. Taken together, jaranol has the potential to effectively treat COVID-19/LUAD by simultaneously targeting multiple genes.

This study provides some new insights as well as potential effective targets of jaranol in the treatment of COVID-19/LUAD for the first time. However, there are still some limitations that need to be addressed. More in vitro and in vivo studies are needed to validate jaranol's underlying mechanisms in the treatment of COVID-19/LUAD. Furthermore, the actual therapeutic benefit is required to be evaluated in clinical COVID-19/LUAD patients.

5. Conclusion

This study elucidated the potential molecular mechanisms of jaranol in the context of treating COVID-19/LUAD through network pharmacology, molecular docking, and CETSA. The identified mechanisms mainly involved eight hub genes and the PI3K/AKT signaling pathway. These findings broadened the therapeutic options for COVID-19/LUAD and offered novel insights for further development of jaranol as a promising pharmaceutical candidate against COVID-19/LUAD.

Funding

This work was supported by the National Natural Science Foundation of China (No. 31601036), Natural Science Foundation of Hubei Province (2021CFB190), Scientific research plan project of Hubei Provincial Department of Education (B2017038), China National College Student Innovation & Entrepreneurship Training Program (202310489017), and Innovation & Entrepreneurship Training Program for College Students of Yangtze University (Yz2022225).

CRediT authorship contribution statement

Zhongcui Kang: Formal analysis, Investigation, Data curation, Writing – original draft. **Qian Wu:** . **Qihang Peng:** Investigation. **Yiting Deng:** Validation. **Hongxia Xu:** Visualization. **Yu Xiao:** Visualization. **Jingda Li:** Writing – review & editing. **Shaobin Li:** Writing – review & editing. **Jin Li:** Supervision, Conceptualization, Writing – review & editing. **Ying Chen:** Supervision.

Declaration of competing interest

The authors declare that they have no known competing financial interests or personal relationships that could have appeared to influence the work reported in this paper.

Appendix A. Supplementary data

Supplementary data to this article can be found online at https://doi.org/10.1016/j.arabjc.2024.105648.

References

Al-Qahtani, A.A., Pantazi, I., Alhamlan, F.S., Alothaid, H., Matou-Nasri, S., Sourvinos, G., Vergadi, E., Tsatsanis, C., 2022. SARS-CoV-2 modulates inflammatory responses of alveolar epithelial type II cells via PI3K/AKT pathway. Front Immunol 13, 1020624. https://doi.org/10.3389/fimmu.2022.1020624.

Andrews, H.S., Herman, J.D., Gandhi, R.T., 2024. Treatments for COVID-19. Annu Rev Med 75, 1. https://doi.org/10.1146/annurev-med-052422-020316.

Appelberg, S., Gupta, S., Svensson Akusjärvi, S., Ambikan, A.T., Mikaeloff, F., Saccon, E., Végvári, Á., Benfeitas, R., Sperk, M., Ståhlberg, M., Krishnan, S., Singh, K., Penninger, J.M., Mirazimi, A., Neogi, U., 2020. Dysregulation in Akt/mTOR/HIF-1 signaling identified by proteo-transcriptomics of SARS-CoV-2 infected cells. Emerg Microbes Infect 9, 1748–1760. https://doi.org/10.1080/22221751.2020.1799723.

Atmaca, A., Wirtz, R.W., Werner, D., Steinmetz, K., Claas, S., Brueckl, W.M., Jäger, E., Al-Batran, S.-E., 2015. SNAI2/SLUG and estrogen receptor mRNA expression are inversely correlated and prognostic of patient outcome in metastatic non-small cell lung cancer. BMC Cancer 15, 300. https://doi.org/10.1186/s12885-015-1310-1.

Basile, M.S., Cavalli, E., McCubrey, J., Hernández-Bello, J., Muñoz-Valle, J.F., Fagone, P., Nicoletti, F., 2022. The PI3K/Akt/mTOR pathway: A potential pharmacological target in COVID-19. Drug Discov Today 27, 848–856. https://doi.org/10.1016/j.drudis.2021.11.002.

Brueckl, W.M., Al-Batran, S.-E., Ficker, J.H., Claas, S., Atmaca, A., Hartmann, A., Rieker, R.J., Wirtz, R.M., 2013. Prognostic and predictive value of estrogen receptor 1 expression in completely resected non-small cell lung cancer. Int J Cancer 133, 1825–1831. https://doi.org/10.1002/ijc.28209.

Chen, J., Li, L.-F., Hu, X.-R., Wei, F., Ma, S., 2021. Network pharmacology-based strategy for elucidating the molecular basis forthe pharmacologic effects of licorice (Glycyrrhiza spp.). Front Pharmacol 12, 590477. https://doi.org/10.3389/fphar.2021.590477.

Daina, A., Michielin, O., Zoete, V., 2019. SwissTargetPrediction: updated data and new features for efficient prediction of protein targets of small molecules. Nucleic Acids Res 47, W357–W364. https://doi.org/10.1093/nar/gkz382.

Elkhalifa, A.E.O., Banu, H., Khan, M.I., Ashraf, S.A., 2023. Integrated Network Pharmacology, Molecular Docking, Molecular Simulation, and In Vitro Validation Revealed the Bioactive Components in Soy-Fermented Food Products and the Underlying Mechanistic Pathways in Lung Cancer. Nutrients 15, 3949. https://doi.org/10.3390/nu15183949.

Fang, S., Dong, L., Liu, L., Guo, J., Zhao, L., Zhang, J., Bu, D., Liu, X., Huo, P., Cao, W., Dong, Q., Wu, J., Zeng, X., Wu, Y., Zhao, Y., 2021. HERB: a high-throughput experiment- and reference-guided database of traditional Chinese medicine. Nucleic Acids Res 49, D1197–D1206. https://doi.org/10.1093/nar/gkaa1063.

Franke, T.F., Yang, S.I., Chan, T.O., Datta, K., Kazlauskas, A., Morrison, D.K., Kaplan, D. R., Tsichlis, P.N., 1995. The protein kinase encoded by the Akt proto-oncogene is a target of the PDGF-activated phosphatidylinositol 3-kinase. Cell 81, 727–736. https://doi.org/10.1016/0092-8674(95)90534-0.

Ge, W., Gong, Y., Li, Y., Wu, N., Ruan, Y., Xu, T., Shu, Y., Qiu, W., Wang, Y., Zhao, C., 2023. IL-17 induces non-small cell lung cancer metastasis via GCN5-dependent SOX4 acetylation enhancing MMP9 gene transcription and expression. Mol Carcinog 62, 1399–1416. https://doi.org/10.1002/mc.23585.

Giaccone, G., Zucali, P.A., 2008. Src as a potential therapeutic target in non-small-cell lung cancer. Ann Oncol 19, 1219–1223. https://doi.org/10.1093/annonc/mdn048.

Hasankhani, A., Bahrami, A., Tavakoli-Far, B., Iranshahi, S., Ghaemi, F., Akbarizadeh, M. R., Amin, A.H., Abedi Kiasari, B., Mohammadzadeh Shabestari, A., 2023. The role of peroxisome proliferator-activated receptors in the modulation of hyperinflammation induced by SARS-CoV-2 infection: A perspective for COVID-19 therapy. Front Immunol 14, 1127358. https://doi.org/10.3389/fimmu.2023.1127358.

Hazra, S., Chaudhuri, A.G., Tiwary, B.K., Chakrabarti, N., 2020. Matrix metallopeptidase 9 as a host protein target of chloroquine and melatonin for immunoregulation in COVID-19: A network-based meta-analysis. Life Sci 257, 118096. https://doi.org/10.1016/j.lfs.2020.118096.

Herrera-Juárez, M., Serrano-Gómez, C., Bote-de-Cabo, H., Paz-Ares, L., 2023. Targeted therapy for lung cancer: Beyond EGFR and ALK. Cancer 129, 1803–1820. https://doi.org/10.1002/cncr.34757.

Kanehisa, M., Furumichi, M., Tanabe, M., Sato, Y., Morishima, K., 2017. KEGG: new perspectives on genomes, pathways, diseases and drugs. Nucleic Acids Res 45, D353–D361. https://doi.org/10.1093/nar/gkw1092.

Keiser, M.J., Roth, B.L., Armbruster, B.N., Ernsberger, P., Irwin, J.J., Shoichet, B.K., 2007. Relating protein pharmacology by ligand chemistry. Nat Biotechnol 25, 197–206. https://doi.org/10.1038/nbt1284.

Khan, S.A., Lee, T.K.W., 2023. Identifying potential pharmacological targets and molecular pathways of Meliae cortex for COVID-19 therapy. Front Immunol 14, 1128164. https://doi.org/10.3389/fimmu.2023.1128164.

Kowalczyk, A., Nisiewicz, M.K., Bamburowicz-Klimkowska, M., Kasprzak, A., Ruzycka-Ayoush, M., Koszytkowska-Stawińska, M., Nowicka, A.M., 2023. Effective voltammetric tool for simultaneous detection of MMP-1, MMP-2, and MMP-9; important non-small cell lung cancer biomarkers. Biosens Bioelectron 229, 115212. https://doi.org/10.1016/j.bios.2023.115212.

Leal, C.M., Leitão, S.G., Sausset, R., Mendonça, S.C., Nascimento, P.H.A., de Araujo, R., Cheohen, C.F., Esteves, M.E.A., Leal da Silva, M., Gondim, T.S., Monteiro, M.E.S., Tucci, A.R., Fintelman-Rodrigues, N., Siqueira, M.M., Miranda, M.D., Costa, F.N., Simas, R.C., Leitão, G.G., 2021. Flavonoids from *Siparuna cristata* as potential inhibitors of SARS-CoV-2 replication. Rev Bras Farmacogn 31, 658–666. https://doi.org/10.1007/s43450-021-00162-5.

Lee, L.Y.W., Cazier, J.-B., Starkey, T., Briggs, S.E.W., Arnold, R., Bisht, V., Booth, S., Campton, N.A., Cheng, V.W.T., Collins, G., Curley, H.M., Earwaker, P., Fittall, M.W., Gennatas, S., Goel, A., Hartley, S., Hughes, D.J., Kerr, D., Lee, A.J.X., Lee, R.J., Lee,

S.M., Mckenzie, H., Middleton, C.P., Murugaesu, N., Newsom-Davis, T., Olsson-Brown, A.C., Palles, C., Powles, T., Protheroe, E.A., Purshouse, K., Sharma-Oates, A., Sivakumar, S., Smith, A.J., Topping, O., Turnbull, C.D., Várnai, C., Briggs, A.D.M., Middleton, G., Kerr, R., UK Coronavirus Cancer Monitoring Project Team, 2020. COVID-19 prevalence and mortality in patients with cancer and the effect of primary tumour subtype and patient demographics: a prospective cohort study. Lancet Oncol 21, 1309–1316. https://doi.org/10.1016/S1470-2045(20)30442-3.

Li, F., Boon, A.C.M., Michelson, A.P., Foraker, R.E., Zhan, M., Payne, P.R.O., 2022. Estrogen hormone is an essential sex factor inhibiting inflammation and immune response in COVID-19. Sci Rep 12, 9462. https://doi.org/10.1038/s41598-022-13585-4.

Ling, W., Li, X., Liu, X., Wu, Q., Wang, W., Meng, J., Sun, B., Lv, B., 2023. Mechanism of the anti-influenza functions of guizhi granules based on network pharmacology, molecular docking, and in vitro experiments. Chem Biodivers 20, e202201228. https://doi.org/10.1002/cbdv.202201228.

Liu, X., Wang, P., Zhang, C., Ma, Z., 2017. Epidermal growth factor receptor (EGFR): A rising star in the era of precision medicine of lung cancer. Oncotarget 8, 50209–50220. https://doi.org/10.18632/oncotarget.16854.

Liu, R., Xu, K.-P., Tan, G.-S., 2015. Cyclooxygenase-2 inhibitors in lung cancer treatment: Bench to bed. Eur J Pharmacol 769, 127–133. https://doi.org/10.1016/j.ejphar.2015.11.007.

Londres, H.D., Armada, J.J., Martínez, A.H., Abdo Cuza, A.A., Sánchez, Y.H., Rodríguez, A.G., Figueroa, S.S., Llanez Gregorich, E.M., Torres Lahera, M.L., Peire, F. G., González, T.M., González, Y.Z., Añé Kouri, A.L., Palomo, A.G., Concepción, M.T., Pérez, L.M., Luaces-Alvarez, P.L., Iglesias, D.E., Hernández, D.S., Suzarte, M.R., Ramos, T.C., 2022. Blocking EGFR with nimotuzumab: a novel strategy for COVID-19 treatment. Immunotherapy 14, 521–530. https://doi.org/10.2217/imt-2022-0027.

Luo, J., Rizvi, H., Preeshagul, I.R., Egger, J.V., Hoyos, D., Bandlamudi, C., McCarthy, C. G., Falcon, C.J., Schoenfeld, A.J., Arbour, K.C., Chaft, J.E., Daly, R.M., Drilon, A., Eng, J., Iqbal, A., Lai, W.V., Li, B.T., Lito, P., Namakydoust, A., Ng, K., Offin, M., Paik, P.K., Riely, G.J., Rudin, C.M., Yu, H.A., Zauderer, M.G., Donoghue, M.T.A., Łuksza, M., Greenbaum, B.D., Kris, M.G., Hellmann, M.D., 2020. COVID-19 in patients with lung cancer. Ann Oncol 31, 1386–1396. https://doi.org/10.1016/j.annonc.2020.06.007.

Matsuyama, T., Kubli, S.P., Yoshinaga, S.K., Pfeffer, K., Mak, T.W., 2020. An aberrant STAT pathway is central to COVID-19. Cell Death Differ 27, 3209–3225. https://doi.org/10.1038/s41418-020-00633-7.

Mazurenko, N.N., Kogan, E.A., Zborovskaya, I.B., Kisseljov, F.L., 1992. Expression of pp60c-src in human small cell and non-small cell lung carcinomas. Eur J Cancer 28, 372–377. https://doi.org/10.1016/s0959-8049(05)80056-5.

Meyer, B., Chiaravalli, J., Gellenoncourt, S., Brownridge, P., Bryne, D.P., Daly, L.A., Grauslys, A., Walter, M., Agou, F., Chakrabarti, L.A., Craik, C.S., Eyers, C.E., Eyers, P. A., Gambin, Y., Jones, A.R., Sierecki, E., Verdin, E., Vignuzzi, M., Emmott, E., 2021. Characterising proteolysis during SARS-CoV-2 infection identifies viral cleavage sites and cellular targets with therapeutic potential. Nat Commun 12, 5553. https://doi.org/10.1038/s41467-021-25796-w.

Mo, J., Tong, Y., Ma, J., Wang, K., Feng, Y., Wang, L., Jiang, H., Jin, C., Li, J., 2023. The mechanism of flavonoids from *Cyclocarya paliurus* on inhibiting liver cancer based on in vitro experiments and network pharmacology. Front Pharmacol 14, 1049953. https://doi.org/10.3389/fphar.2023.1049953.

Mondal, S., Adhikari, N., Banerjee, S., Amin, S.A., Jha, T., 2020. Matrix metalloproteinase-9 (MMP-9) and its inhibitors in cancer: A minireview. Eur J Med Chem 194, 112260. https://doi.org/10.1016/j.ejmech.2020.112260.

Moustaqil, M., Ollivier, E., Chiu, H.-P., Van Tol, S., Rudolffi-Soto, P., Stevens, C., Bhumkar, A., Hunter, D.J.B., Freiberg, A.N., Jacques, D., Lee, B., Sierecki, E., Gambin, Y., 2021. SARS-CoV-2 proteases PLpro and 3CLpro cleave IRF3 and critical modulators of inflammatory pathways (NLRP12 and TAB1): implications for disease presentation across species. Emerg Microbes Infect 10, 178–195. https://doi.org/10.1080/22221751.2020.1870414.

Niu, M., Zhang, B., Li, L., Su, Z., Pu, W., Zhao, C., Wei, L., Lian, P., Lu, R., Wang, R., Wazir, J., Gao, Q., Song, S., Wang, H., 2021. Targeting HSP90 inhibits proliferation and induces apoptosis through AKT1/ERK pathway in lung cancer. Front Pharmacol 12, 724192. https://doi.org/10.3389/fphar.2021.724192.

Passos, F.R.S., Heimfarth, L., Monteiro, B.S., Corrêa, C.B., de Moura, T.R., de Araújo, A. A., S., Martins-Filho, P.R., Quintans-Júnior, L.J., Quintans, J. de S.S.,, 2022. Oxidative stress and inflammatory markers in patients with COVID-19: Potential role of RAGE, HMGB1, GFAP and COX-2 in disease severity. Int Immunopharmacol 104, 108502. https://doi.org/10.1016/j.intimp.2021.108502.

Perico, N., Cortinovis, M., Suter, F., Remuzzi, G., 2023. Home as the new frontier for the treatment of COVID-19: the case for anti-inflammatory agents. Lancet Infect Dis 23, e22–e33. https://doi.org/10.1016/S1473-3099(22)00433-9.

Reddy, A.T., Lakshmi, S.P., Reddy, R.C., 2016. PPARγ as a Novel Therapeutic Target in Lung Cancer. PPAR Res 2016, 8972570. https://doi.org/10.1155/2016/8972570.

Ru, J., Li, P., Wang, J., Zhou, W., Li, B., Huang, C., Li, P., Guo, Z., Tao, W., Yang, Y., Xu, X., Li, Y., Wang, Y., Yang, L., 2014. TCMSP: a database of systems pharmacology for drug discovery from herbal medicines. J Cheminform 6, 13. https://doi.org/10.1186/1758-2946-6-13.

Sanaei, M.-J., Razi, S., Pourbagheri-Sigaroodi, A., Bashash, D., 2022. The PI3K/Akt/mTOR pathway in lung cancer; oncogenic alterations, therapeutic opportunities, challenges, and a glance at the application of nanoparticles. Transl Oncol 18, 101364. https://doi.org/10.1016/j.tranon.2022.101364.

Savic, G., Stevanovic, I., Mihajlovic, D., Jurisevic, M., Gajovic, N., Jovanovic, I., Ninkovic, M., 2022. MMP-9/BDNF ratio predicts more severe COVID-19 outcomes. Int J Med Sci 19, 1903–1911. https://doi.org/10.7150/ijms.75337.

Shi, S., Yu, G., Huang, B., Mi, Y., Kang, Y., Simon, J.P., 2020. PPARG could work as a valid therapeutic strategy for the treatment of lung squamous cell carcinoma. PPAR Res 2020, 2510951. https://doi.org/10.1155/2020/2510951.

Sung, H., Ferlay, J., Siegel, R.L., Laversanne, M., Soerjomataram, I., Jemal, A., Bray, F., 2021. Global Cancer Statistics 2020: GLOBOCAN estimates of incidence and mortality worldwide for 36 cancers in 185 countries. CA: A Cancer Journal for Clinicians 71, 209–249. https://doi.org/10.3322/caac.21660.

Tan, A.C., 2020. Targeting the PI3K/Akt/mTOR pathway in non-small cell lung cancer (NSCLC). Thorac Cancer 11, 511–518. https://doi.org/10.1111/1759-7714.13328.

Tang, J.-M., He, Q.-Y., Guo, R.-X., Chang, X.-J., 2006. Phosphorylated Akt overexpression and loss of PTEN expression in non-small cell lung cancer confers poor prognosis. Lung Cancer 51, 181–191. https://doi.org/10.1016/j.lungcan.2005.10.003.

Tomazou, M., Bourdakou, M.M., Minadakis, G., Zachariou, M., Oulas, A., Karatzas, E., Loizidou, E.M., Kakouri, A.C., Christodoulou, C.C., Savva, K., Zanti, M., Onisiforou, A., Afxenti, S., Richter, J., Christodoulou, C.G., Kyprianou, T., Kolios, G., Dietis, N., Spyrou, G.M., 2021. Multi-omics data integration and network-based analysis drives a multiplex drug repurposing approach to a shortlist of candidate drugs against COVID-19. Brief Bioinform 22, bbab114. https://doi.org/10.1093/bib/bbab114.

Ueland, T., Holter, J.C., Holten, A.R., Müller, K.E., Lind, A., Bekken, G.K., Dudman, S., Aukrust, P., Dyrhol-Riise, A.M., Heggelund, L., 2020. Distinct and early increase in circulating MMP-9 in COVID-19 patients with respiratory failure. J Infect 81, e41–e43. https://doi.org/10.1016/j.jinf.2020.06.061.

Wang, X., Shen, Y., Wang, S., Li, S., Zhang, W., Liu, X., Lai, L., Pei, J., Li, H., 2017. PharmMapper 2017 update: a web server for potential drug target identification with a comprehensive target pharmacophore database. Nucleic Acids Res 45, W356–W360. https://doi.org/10.1093/nar/gkx374.

Wang, Y., Schughart, K., Pelaia, T.M., Chew, T., Kim, K., Karvunidis, T., Knippenberg, B., Teoh, S., Phu, A.L., Short, K.R., Iredell, J., Thevarajan, I., Audsley, J., Macdonald, S., Burcham, J., Predict-Consortium, null, Tang, B., McLean, A., Shojaei, M., 2023. Pathway and Network Analyses Identify Growth Factor Signaling and MMP9 as Potential Mediators of Mitochondrial Dysfunction in Severe COVID-19. Int J Mol Sci 24, 2524. https://doi.org/10.3390/ijms24032524.

Wang, Qihui, Zhang, Y., Wu, L., Niu, S., Song, C., Zhang, Z., Lu, G., Qiao, C., Hu, Y., Yuen, K.-Y., Wang, Qisheng, Zhou, H., Yan, J., Qi, J., 2020. Structural and Functional Basis of SARS-CoV-2 Entry by Using Human ACE2. Cell 181, 894–904.e9. https://doi.org/10.1016/j.cell.2020.03.045.

Woo, J.-H., Ahn, J.-H., Jang, D.S., Lee, K.-T., Choi, J.-H., 2017. Effect of kumatakenin isolated from cloves on the apoptosis of cancer cells and the alternative activation of tumor-associated macrophages. J. Agric. Food Chem. 65, 7893–7899. https://doi.org/10.1021/acs.jafc.7b01543.

World Health Organization, 2023. WHO Coronavirus (COVID-19) Dashboard. accessed September 21, 2023. https://covid19.who.int/.

Wu, C., Liu, Y., Yang, Y., Zhang, P., Zhong, W., Wang, Y., Wang, Q., Xu, Y., Li, M., Li, X., Zheng, M., Chen, L., Li, H., 2020. Analysis of therapeutic targets for SARS-CoV-2 and discovery of potential drugs by computational methods. Acta Pharm Sin B 10, 766–788. https://doi.org/10.1016/j.apsb.2020.02.008.

Wu, Y., Zhang, F., Yang, K., Fang, S., Bu, D., Li, H., Sun, L., Hu, H., Gao, K., Wang, W., Zhou, X., Zhao, Y., Chen, J., 2019. SymMap: an integrative database of traditional Chinese medicine enhanced by symptom mapping. Nucleic Acids Res 47, D1110–D1117. https://doi.org/10.1093/nar/gky1021.

Xu, H.-Y., Zhang, Y.-Q., Liu, Z.-M., Chen, T., Lv, C.-Y., Tang, S.-H., Zhang, X.-B., Zhang, W., Li, Z.-Y., Zhou, R.-R., Yang, H.-J., Wang, X.-J., Huang, L.-Q., 2019. ETCM: an encyclopaedia of traditional Chinese medicine. Nucleic Acids Res 47, D976–D982. https://doi.org/10.1093/nar/gky987.

Yuan, Y., Du, W., Wang, Y., Xu, C., Wang, J., Zhang, Y., Wang, H., Ju, J., Zhao, L., Wang, Z., Lu, Y., Cai, B., Pan, Z., 2015. Suppression of AKT expression by miR-153 produced anti-tumor activity in lung cancer. Int J Cancer 136, 1333–1340. https://doi.org/10.1002/ijc.29103.

Yuen, C.-K., Wong, W.-M., Mak, L.-F., Wang, X., Chu, H., Yuen, K.-Y., Kok, K.-H., 2021. Suppression of SARS-CoV-2 infection in ex-vivo human lung tissues by targeting class III phosphoinositide 3-kinase. J Med Virol 93, 2076–2083. https://doi.org/10.1002/jmv.26583.

Zhang, Q., Huang, X., 2021. The modulatory properties of *Astragalus membranaceus* treatment on endometrial cancer: an integrated pharmacological method. PeerJ 9, e11995.

Zhao, Z., Xu, L.-D., Zhang, F., Liang, Q.-Z., Jiao, Y., Shi, F.-S., He, B., Xu, P., Huang, Y.-W., 2023. Heat shock protein 90 facilitates SARS-CoV-2 structural protein-mediated virion assembly and promotes virus-induced pyroptosis. J Biol Chem 299, 104668. https://doi.org/10.1016/j.jbc.2023.104668.

Zhou, Y., Zhou, B., Pache, L., Chang, M., Khodabakhshi, A.H., Tanaseichuk, O., Benner, C., Chanda, S.K., 2019. Metascape provides a biologist-oriented resource for the analysis of systems-level datasets. Nat Commun 10, 1523. https://doi.org/10.1038/s41467-019-09234-6.